

PRODUCTION OF $Y^0(\Lambda, \Sigma^0)$ AND K^0 PARTICLES ON LIGHT NUCLEI BY 2.8-Bev/c PIONS

Ya. Ya. SHALAMOV, V. A. SHEBANOV, and A. F. GRASHIN

Institute of Theoretical and Experimental Physics, Academy of Sciences, U.S.S.R.

Submitted to JETP editor December 29, 1960

J. Exptl. Theoret. Phys. (U.S.S.R.) 40, 1302-1312 (May, 1961)

The production of $Y^0(\Lambda, \Sigma^0)$ hyperons and K^0 mesons by 2.8-Bev/c π^- mesons on light nuclei was studied in a freon ($C_2F_5Cl_3$) bubble chamber. The Y^0 and K^0 production cross sections are $(2.5 \pm 0.5)\%$ and $(7 \pm 1)\%$ respectively of the total cross section for inelastic processes. The cross sections for these processes, as well as the angular and momentum distributions of the particles produced, were determined from 143 $Y^0 + K^0$ and $K^0 + \bar{K}^0$ production events. The ratio of the cross section is $\sigma(K^0\bar{K}^0)/\sigma(Y^0K^0) = 0.65 \pm 0.15$ and their sum is $\sigma(K^0\bar{K}^0) + \sigma(Y^0K^0) = (3.2 \pm 0.8)\%$ of the total cross section for inelastic processes. 80–90% of the $Y^0 + K^0$ production events are accompanied by a π -meson production, but in 70–80% of the $K^0 + \bar{K}^0$ production events, no π meson is emitted.

A characteristic feature is that, in the $K^0 + \bar{K}^0$ production, the K^0 mesons carry off practically all of the available energy, whereas a soft hyperon spectrum is observed in $Y^0 + K^0$ production events.

The cross section for the reactions $\pi^- + \pi^+ \rightarrow K^0 + \bar{K}^0$ ($\sigma \sim 2$ mb) and $\pi^- + K^{0,+} \rightarrow \pi^{-,0} + K^0$ ($\sigma \gtrsim 10$ mb) can be estimated for final kinetic energies of the particles in the c.m.s. ≤ 0.5 Bev by assuming that, in the reaction under consideration, the pole diagrams make a large contribution, at least for small transferred momenta.

DETAILED experimental data have become available on the production of strange particles in π^-p collisions near the threshold in the 0.9–1.3 Bev energy range.^{1,2} The production of $Y^0(\Lambda, \Sigma^0)$ hyperons and K^0 mesons in collisions of π mesons with nuclei has been studied at 1.5 and 1.9 Bev.³⁻⁵

Kuznetsov et al.⁶ measured the ratio of the cross sections $\sigma(K^0\bar{K}^0)/[\sigma(\Lambda K^0) + \sigma(\Sigma^0 K^0)] = 0.51 \pm 0.19$ for the xenon nucleus at 2.8-Bev/c π^- -meson momentum. The production of strange particles in π^-p collisions has been studied at 6.8 Bev/c.⁷

In the present experiment, the production of $Y^0(\Lambda, \Sigma^0)$ hyperons and K^0 mesons on carbon, fluorine, and chlorine nuclei by π^- mesons with 2.8-Bev/c momentum was studied. The experiment was carried out by means of a 17-liter freon bubble chamber⁸ using the external π^- -meson beam of the proton synchrotron at the High-Energy Laboratory of the Joint Institute for Nuclear Research.

EXPERIMENTAL METHOD

In the experiments with the 2.8-Bev/c π^- -meson beam (momentum spread $\Delta p/p = 10\%$), about 60 000 stereoscopic photographs were obtained using the freon ($C_2F_5Cl_3$) bubble chamber

without magnetic field.⁸ All photographs were scanned by two independent observers. In the scanning, those interactions of π^- mesons with nuclei that were accompanied by V decays correlated with the point of interaction were selected. These correspond to the decays $\Lambda \rightarrow p + \pi^-$ or $K^0 \rightarrow \pi^+ + \pi^-$. About 2000 such events were found. Out of these, 149 were accompanied by double V decays. After the analysis of these events, six were considered as background events because of the noncoplanarity of one of the V decays with the point of interaction. The remaining 143 events were identified as associated particle production $Y^0(\Lambda, \Sigma^0) + K^0$ or $K^0 + \bar{K}^0$. These events were then analyzed in detail, as well as that part of the data which enables us to obtain information on the total production cross section of Y^0 and K^0 particles on nuclei. It should be noted that we did not differentiate experimentally between the events of Λ and Σ^0 production, but the total yield for the $Y^0(\Lambda, \Sigma^0)$ hyperons was found.

The spatial analysis of the photographs was carried out with a stereo-projector, by means of which the coplanarity was checked, and the angles of emission and the particle ranges were measured. The decay particles were identified by a kinematic analysis of the angles between the direc-

tion of motion of the V particles and of their decay products, by range and ionization measurements, and from the multiple scattering of particles in the working liquid of the chamber. Out of 101 detected events of associated production of Y^0 and K^0 particles, 41 Λ hyperons were identified from the angles of emission of the particles and their ranges (mainly from the proton ranges), 42 Λ hyperons were identified from the angles and the ionization J of protons at $J \geq 2J_{\min}$, 13 Λ hyperons from the angles and ionization at $J \sim 1.5 \times J_{\min}$, and 5 Λ hyperons from the energy and momentum conservation laws.

The momenta of the Λ and K^0 particles were determined from calculated kinematic relations between the angles of emission of the decay products, using the tables of Leipuner.⁹ The accuracy of the momentum measurements was determined by the measurement accuracy for the emission angles of the decay products of Λ and K^0 particles, and amounted to about 10% on the average. In order to find the absolute yield of Y^0 and K^0 particles, the total number of interactions of π^- mesons in the working volume of the chamber was counted, and a correction was applied to the number of detected Λ and K^0 particles. In the correction, the following factors were taken into account: the fractions of Λ and K^0 particles decaying into neutral particles, the fraction of long-lived K^0 mesons, the geometrical coefficients α_1 and α_2 , and the fractions of Λ and K^0 decay events that were not detected in the chamber either because of the short range of the decay products or because of relatively small emission angles. (In the latter case, the decays might be imitated by high-energy electron-positron pairs.)

The geometrical coefficient α_1 is determined by the detection probability of Λ and K^0 particles in the effective volume, and is given by the equation $\alpha_1^{-1} = 1 - \exp(-L/L_0)$, where L is the "potential" range of Λ and K^0 particles and L_0 is the decay mean free path. The mean value $\bar{\alpha}_1$ was found to be equal to 1.16 for Λ particles and 1.20 for K^0 particles.

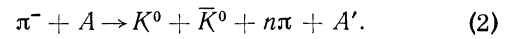
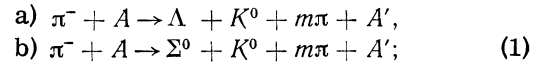
The coefficient α_2 is related to the decreased detection efficiency of V decays in the plane perpendicular to the plane photographed. It is determined experimentally and is, on the average, equal to 1.15 ± 0.08 both for Λ and K^0 particles.

The resulting values of the correction factors used to multiply the number of Λ and of K^0 particles detected in the chamber are 2.70 and 4.20 respectively.

EXPERIMENTAL RESULTS

1. Cross Section for the Production of the Particle Pairs $Y^0 + K^0$ and $K^0 + \bar{K}^0$, and Total Cross Section for the Production of Y^0 and K^0 Particles

The associated production processes $Y^0 + K^0$ and $K^0 + \bar{K}^0$ on nuclei were studied in the following reactions:



The measurements did not differentiate between reactions (1a) and (1b), and therefore the total cross section σ_1 for the associated production $Y + K^0$ and $\Sigma^0 + K^0$ was measured.

Out of 143 events of the associated production $Y^0 + K^0$ and $K^0 + \bar{K}^0$, 101 (5) events were considered as $Y^0 + K^0$, and 42 (4) as $K^0 + \bar{K}^0$. (The figures in the parentheses refer to the number of doubtful cases, in which no clear choice between $Y^0 + K^0$ and $K^0 + \bar{K}^0$ could be made.) The ratio of the cross sections for reactions (2) and (1) calculated from these events is $\sigma_2/\sigma_1 = 0.65 \pm 0.15$; the undetermined cases have been taken into account in calculating the error. The value obtained is in agreement, within the limits of experimental error, with the value for the xenon nucleus 0.51 ± 0.19 given by Kuznetsov et al.⁶ for the same π^- -meson energy. The total cross section $\sigma_1 + \sigma_2$ amounts to $(3.2 \pm 0.8)\%$ of the total cross section for inelastic interactions of π^- mesons with fluorine nuclei. In calculating the results, it was assumed that the cross section per nucleus varies little between the lightest nucleus (C) and the heaviest one (Cl) of the mixture.

A rough estimate of the cross section for the production of the $K^0 + \bar{K}^0$ and $Y^0 + K^0$ pairs per nucleon gives $\sigma'(K^0\bar{K}^0) \approx \sigma'(Y^0K^0) \approx 0.5$ mb. The large value of the cross section for the production of $K^0 + \bar{K}^0$ pairs at 2.65-Bev π^- -meson energy indicates a fast increase in this cross section with increasing energy of the π^- mesons above 1.5 Bev. (No production of $K^0\bar{K}^0$ pairs is observed at 1.5 Bev.³)

The total cross section for the production of Y^0 and K^0 particles was obtained by a triple scanning of about 3000 pictures. A total of 8015 interactions of π^- mesons with nuclei, 73 events of Y^0 -particle production, and 143 events of K^0 -particle production were detected in these pictures. The

total yield of $Y^0(\Lambda, \Sigma^0)$ hyperons amounted to $(2.5 \pm 0.5)\%$ and the yield of K^0 mesons to $(7 \pm 1)\%$, relative to the total cross section for inelastic interactions of π^- mesons with nuclei. From a comparison of these results with the data for carbon at 1.5-Bev π^- -meson energy,³ i.e., (1.7 ± 0.4) and $(1.4 \pm 0.5)\%$ for Y^0 and K^0 particles respectively, it is clear that the yield of Y^0 hyperons is greater by a factor of 1.5, and that of K^0 mesons by a factor of five.

In order to determine the value of m and n in reactions (1) and (2), an analysis of the stars correlated with a given pair of strange particles was carried out. The most reliable result is given by the analysis according to the number of γ rays accompanying the production of strange particles. For the Y^0 -hyperon production, this number, as determined from 30 conversion events $\gamma \rightarrow e^+ + e^-$ for the $Y^0 + K^0$ process and from 85 events for the $Y^0 + K^+, 0$ process was found to equal $n_\gamma(Y^0 K^0) = 1.0 \pm 0.15$. For the $K^0 + \bar{K}^0$ production, the value found from three events is $n_\gamma(K^0 \bar{K}^0) = 0.22 \pm 0.15$. The number of π^0 mesons is therefore equal to $n_{\pi^0}(Y^0 K^0) \leq 0.5 \pm 0.07$ and $n_{\pi^0}(K^0 \bar{K}^0) = 0.11 \pm 0.07$. The inequality sign in the first case is due to the possible detection of electron-positron pairs produced as a result of the conversion of γ rays from the $\Sigma^0 \rightarrow \Lambda + \gamma$ decays. The number of charged mesons in stars was determined from the number of particles having a relativistic ionization. The total mean number of π mesons in the reactions (1) and (2) is equal to $m = 1.2 \pm 0.15$ and $n = 0.6 \pm 0.15$.

2. Angular and Momentum Distribution

The angular and momentum distributions for Λ and K^0 particles are shown in Fig. 1. The angular distributions of Λ and K^0 particles in the labora-

tory system (l.s.) are strongly peaked forward: 80–90% of the particles are within a cone with $\cos \theta \geq 0.8$. The momentum spectrum of Λ particles was studied at $p_\Lambda \geq 300$ Mev/c and the spectra of K^0 mesons at $p_{K^0} \geq 100$ Mev/c. The spectrum of Λ particles has a maximum at 600 Mev/c and decreases rapidly at higher momenta. The spectra of K^0 mesons in both reactions have a maximum for $p_{K^0} \approx 1$ Bev/c and continue up to 2.5 Bev/c. An estimate of possible distortions of the momentum spectra caused by a difference in the correction factors for different momentum values was carried out. The difference, however, was not greater than 10–15%, and it was therefore neglected. The possibility of determining the momentum of Σ^0 particles by measuring the momenta of Λ particles in the $\Sigma^0 \rightarrow \Lambda + \gamma$ decay was analyzed. The distortion of the Σ^0 spectrum caused by this decay is negligible, and, in our case, amounts to 4–7% depending on the Σ^0 momentum. Therefore, the momentum spectrum of the Λ hyperons is henceforth considered as a total spectrum of the $Y^0(\Lambda, \Sigma^0)$ hyperons.

An interesting result was obtained in considering the total kinetic energy carried away by the two K^0 mesons in $K^0 + \bar{K}^0$ production events. In Fig. 2, each $K^0 + \bar{K}^0$ production event is denoted by a rectangle with a number showing the number of prongs in the star. In the figure, the arrow denotes the available energy corresponding to the energy of the π^- -meson beam, and limits determined by its energy half-width are shown. The mean energy in the spectrum is $\bar{T} = 1.30$ Bev. The mean energy of the $K^0 + \bar{K}^0$ production events is greater than this value because of inelastic interactions of K^0 mesons in nuclei. If we consider the distribution of the energy carried away by K^0 mesons in prong-

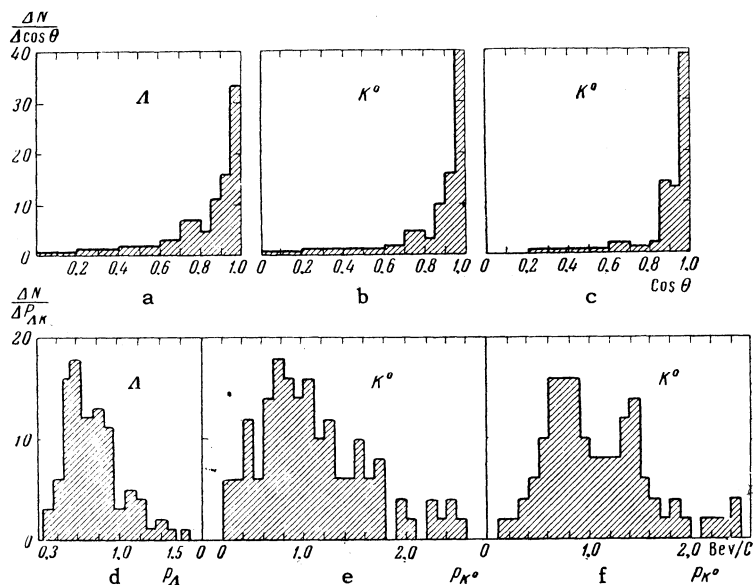


FIG. 1. Angular and momentum distributions for Λ and K^0 particles in the l.s. a, b, d, e – for reactions (1); c, f – for reactions (2).

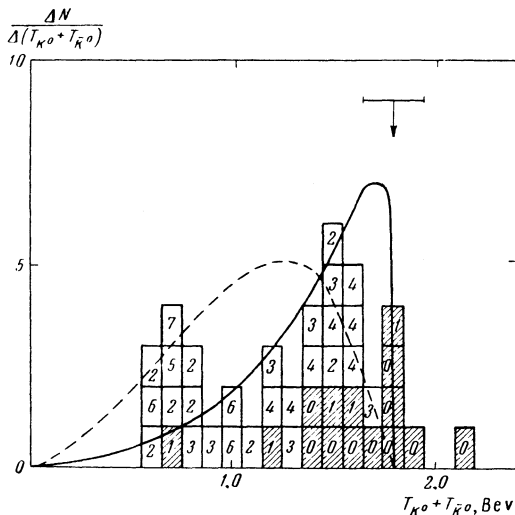


FIG. 2. Distribution of the total kinetic energy T carried away by K^0 and \bar{K}^0 mesons in the 1.s. The dotted and solid lines represent the theoretical curves for the phase volume and for the polar diagrams of Fig. 4 respectively.

less and one-prong stars (the shaded rectangles in Fig. 2), for which we can assume a relatively small energy loss by K^0 mesons as a result of the inelastic collisions, then the mean value of the energy carried away by the two K^0 mesons is found to be 1.60 BeV. Thus, the characteristic feature of the associated production of $K^0 + \bar{K}^0$ is the large value of the energy carried away by the K mesons, close to the limiting value. The total uncertainty in the energy of two K^0 mesons carried away in a $K^0 + \bar{K}^0$ associated production event, in addition to the uncertainty in the energy of the π^- -meson beams, is determined only by the accuracy of the K^0 -meson energy measurement and by the Fermi width of the momenta of nucleons taking part in the production of $K^0 + \bar{K}^0$, and, in our case, amounts to ± 0.25 BeV. This means, in particular, that if the energy carried away by the K^0 mesons in a $K^0 + \bar{K}^0$ event is equal to the limiting value, then all events will have a distribution with an energy width of 0.5 BeV.

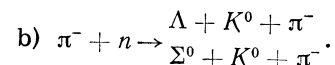
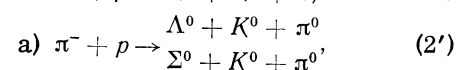
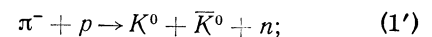
3. Mean Number of π Mesons Accompanying the Elementary Act of Production of $Y^0 + K^0$ and $K^0 + \bar{K}^0$

In the determination of the cross sections and of the features of particle production from data obtained on light nuclei, a considerable uncertainty is introduced by the contributions of the nucleus. Nevertheless, it is possible to study a number of features of the elementary processes for a given π^- -meson energy. In order to estimate the influence of the nucleus, calculations based on the optical model were carried out,

using a simplified one-dimensional model. Calculations carried out for the fluorine nucleus (the average nucleus of the freon mixture) show that 1) about 70% of Λ hyperons produced in the nucleus do not interact with nuclear matter, and 2) 15–20% of K^0 and 30–40% of \bar{K}^0 mesons undergo inelastic interactions in the nucleus. The following values were used in the calculations: mean free path of π^- meson in nuclear matter $\lambda_\pi = 4 \times 10^{-13}$ cm, cross section $\sigma(\Lambda + N) \approx 30 - 40$ mb, cross sections $\sigma(K^0 + N)$ and $\sigma(\bar{K}^0 + N)$ for the mean K^0 -particle momentum of 1.1 BeV/c are 17 and 40 mb respectively, similarly as for $K^+ + N$ and $K^- + N$ events, according to the data of Crawford et al.¹⁰

Taking into account the fraction of inelastic interactions of K^0 and \bar{K}^0 mesons in nuclei calculated according to the optical model, and knowing the average number of π mesons produced as a result of inelastic collisions, we can estimate the number of secondary mesons in reactions (1) and (2), m_1 and n_1 . The average number of π mesons produced per inelastic interaction of K^0 and \bar{K}^0 mesons in a nucleus was determined from preliminary experimental data obtained in an experiment using the same bubble chamber (altogether 20 events of such interactions were observed), and amounts to 1.0 ± 0.25 . Hence, we obtain the estimate $m_1 = 0.2$, $n_1 = 0.5 - 0.6$ and, consequently, the total number of π mesons produced in an associated production event $Y^0 + K^0$ and $K^0 + \bar{K}^0$ is, on the average, equal to $m' = 1 \pm 0.2$ and $n' = 0.0 \pm 0.3$ respectively.

The results obtained show that the production of Y^0 hyperons in π^-N collisions of 2.8-BeV/c π^- mesons is, in 80–90% of the events, accompanied by the production of a π meson, while the production of a $K^0 + \bar{K}^0$ pair is, in 70–80% of the cases, not accompanied by an emission of a π meson. Thus, the production of the $K^0\bar{K}^0$ and Y^0K^0 pairs on nucleons in a nucleus evidently occurs mainly in the following elementary reactions:



Additional information on the elementary reactions on nucleons in a nucleus were obtained by analyzing the prongless stars accompanying the $Y^0 + K^0$ and $K^0 + \bar{K}^0$ production events. For the first case, 20 (out of 101) such events were found, and in 8 of these electron-positron pairs were de-

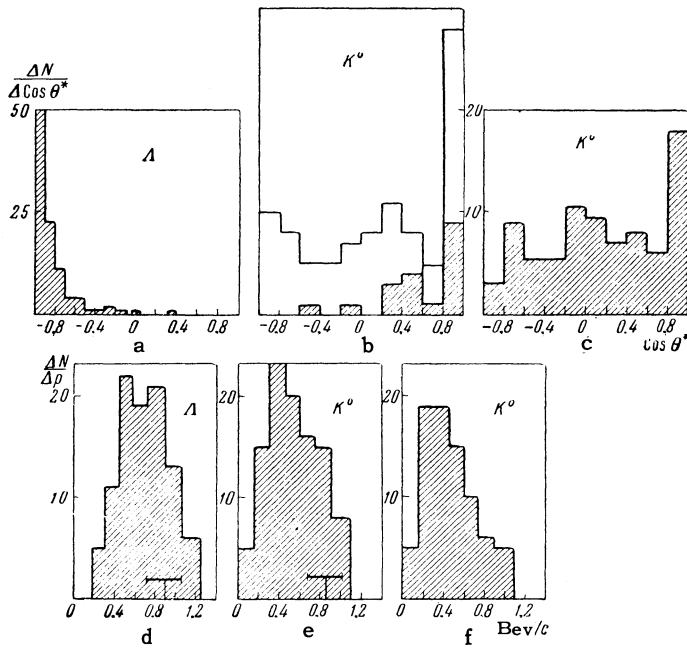


FIG. 3. Angular and momentum distributions of Y^0 and K^0 particles in the pion-nucleon c.m.s.: a, b, d, e – for cases of associated production of $Y^0 + K^0$, and c, f – for $K^0 + \bar{K}^0$ pairs. In the spectra d and e the limiting values of momenta obtained taking the Fermi motion of nucleons in the nucleus into account are indicated.

ected originating in the photon conversion correlated with the prongless star. (In one case, there were two such pairs present.) If we assume that in all of these 20 events a reaction of the type (2')a occurred, then we should observe 8–10 π^0 mesons in the chamber, which was actually the case in the experiment. Unfortunately, it is impossible to estimate the relative contribution of the reaction involving the Σ^0 hyperon from the data. For the second case ($K^0 + \bar{K}^0$ pairs), 10 prongless stars (out of 42) that were not accompanied by electron-positron pairs, according to reaction (1'), were observed. If, in the production of $K^0 + \bar{K}^0$, one π^0 meson was present, we would detect 4–5 events in which prongless stars are accompanied by electron-positron pairs.

4. Angular and Momentum Distributions of Y^0 and K^0 Particles in the Pion-Nucleon C.M.S.

Under the assumption that the production of $Y^0 + K^0$ and $K^0 + \bar{K}^0$ pairs occurs in π -N collisions, and neglecting secondary interactions of Y^0 and K^0 particles in nuclei, we have obtained the angular and momentum distributions of Y^0 and K^0 particles in the c.m.s. (see Fig. 3). In this system, all Y^0 particles propagate into the backward hemisphere, with a very large fraction of the particles (> 80%) being contained in a cone

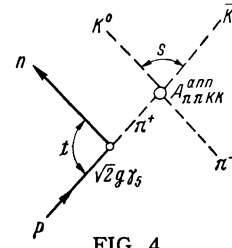


FIG. 4

with $\cos \theta^* \leq -0.8$. The angular distribution of K^0 particles produced together with the Y^0 particles is peaked forward. This is especially noticeable for prongless stars, whose distribution is shown shaded in the figure. The forward direction of the total momentum of the two K^0 mesons is characteristic for the production process $K^0 + \bar{K}^0$ (the forward-backward relation is equal to 3.3 ± 0.8). In all prongless stars, the total momentum of the two K^0 mesons is directed forwards only.

ESTIMATES OF THE $\pi\pi KK$ FOUR-BRANCH VERTEX FROM OBSERVED EXPERIMENTAL DATA

The experimental data obtained shows that, in reactions (1') and (2'), the final baryons have a relatively small energy in the l.s., which corresponds to small transferred momentum

$$-t = 2m_N(\omega - m) - (m - m_N)^2,$$

where ω and m are the total energy in the l.s. and the baryon mass respectively, and m_N is the nucleon mass.

From general theoretical considerations,¹¹⁻¹³ we can expect that, for a small momentum transfer, the main contribution to the reactions (1') and (2') is due to single-meson pole diagrams, shown in Figs. 4 and 5. For the same reason, a comparison of theoretical predictions for the momentum spectrum with experimental data in the range of small t should enable us to find the annihilation cross section

$$\pi^- + \pi^+ \rightarrow K^0 + \bar{K}^0 \quad (3)$$

and the scattering cross section

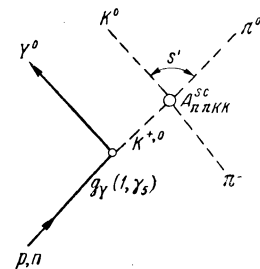


FIG. 5

$$\pi^- + K^{0,+} \rightarrow \pi^{-,0} + K^0 \quad (4)$$

from the data on reactions (1') and (2') respectively. However, the data on the baryon spectra is very poor, and does not permit us to use the extrapolation method of Chew and Low.¹¹ Instead, it is possible to compare the integral cross sections in a certain part of the spectrum corresponding to a small momentum transfer, which is equivalent to the consideration of the sum of partial cross sections with large orbital momenta.^{12,13}

As will be seen in the following discussion, it is necessary to consider a relatively large part of the spectrum in which diagrams without poles should, in general, make the same contribution as pole diagrams. Although it is difficult at present to obtain any reliable estimate of the validity of the approximation made, we can assume that the values obtained for the cross sections for the reactions (3) and (4) are correct at least to within one order of magnitude.

For the process (1'), the polar approximation gives the laboratory neutron spectrum in the form

$$d\sigma = 2g^2 \frac{|t|}{(t - \mu^2)^2} \int_{4\mu_h^2}^{s_m(\omega)} \sqrt{(s - 4\mu^2)s} \sigma_{\pi^- \pi^+}^{\text{ann}}(s) ds \frac{d\omega}{8\pi m p_0^2},$$

where

$$\sigma_{\pi^- \pi^+}^{\text{ann}}(s) = \frac{4}{s} \sqrt{\frac{s - 4\mu_h^2}{s - 4\mu^2}} \int |A_{\pi\pi KK}^{\text{ann}} / 16\pi|^2 d\Omega_{\text{ann}}, \quad (5)$$

$$s_m(\omega) = 2p_0 \sqrt{\omega^2 - m^2} - 2(\omega - m)(m + \omega_0) + \mu^2, \\ t = -2m(\omega - m),$$

where μ and μ_K are the masses of the π and K mesons, p_0 and ω_0 are the momentum and energy of the incident π meson in the l.s., $g^2 = 14.5$, $\sigma_{\pi\pi}^{\text{ann}}(s)$ is the cross section for the process (3) as a function of the square of the energy s in the c.m.s. for the same process, and s_m is the maximum possible value of s for a given energy ω of the recoil neutron.

We shall assume that the square of the invariant matrix element $A_{\pi\pi KK}^{\text{ann}}$ ($\pi\pi KK$ is the four-branch vertex in the annihilation channel) averaged over the angles does not produce an additional dependence on s , i.e., we shall assume that $\int |A_{\pi\pi KK}^{\text{ann}}|^2 d\Omega_{\text{ann}} = \text{const}$. In this case, in addition to the factor $t/(t - \mu^2)^2$ from the vertex $NN\pi$, the laboratory spectrum is determined only by the invariant phase volume of the final particles

$$\int \Phi(\omega) d\omega = \int \frac{dp}{\omega} \frac{dp_1}{\omega} \frac{dp_2}{\omega} \delta(\Sigma p). \quad (6)^*$$

If the masses of all particles are different, then

*Arth = \tanh^{-1} .

$$\Phi(\omega) = \frac{2\pi^2}{p_0} \left\{ \sqrt{[s_m - (\mu_1 + \mu_2)^2][s_m - (\mu_1 - \mu_2)^2]} \right. \\ \left. - 2(\mu_1^2 + \mu_2^2) \text{Arth} \sqrt{\frac{s_m - (\mu_1 + \mu_2)^2}{s_m - (\mu_1 - \mu_2)^2}} \right. \\ \left. + 2(\mu_1^2 - \mu_2^2) \text{Arth} \left(\frac{\mu_1 - \mu_2}{\mu_1 + \mu_2} \sqrt{\frac{s_m - (\mu_1 + \mu_2)^2}{s_m - (\mu_1 - \mu_2)^2}} \right) \right\} \quad (6')$$

where $s_m = 2p_0 \sqrt{\omega^2 - m^2} + m^2 + m_0^2 + \mu_0^2 + 2m_0\omega_0 - 2\omega(m_0 + \omega_0)$, p_0 and ω_0 are the momentum and energy of the incident particle in the l.s., m_0 is the mass of the target, ω and m are the energy and mass of the particle under consideration in the l.s., and μ_1 and μ_2 are the masses of the two other final particles.*

The theoretical distributions of the kinetic energy of two K^0 mesons in the l.s., $T = \omega_0 - m_N - \omega - 2\mu_K$, are shown in Fig. 2 [the dotted line represents the normalized curve of the phase space (6')]. If we consider the experimental spectrum obtained from prongless and one-prong stars (where the distortions from the interaction of K^0 mesons in the nucleus are at a minimum), then we can conclude that there is a qualitative agreement between the theoretical curve and the experiment.†

In such a case, the comparison of integral cross sections over different parts of the spectrum leads roughly to the same values of the $\pi\pi KK$ four-branch vertex. Because of this, we shall integrate the theoretical spectrum over the interval $\Delta T = 0 - 0.5$ Bev ($|t| \leq m_N^2$), and shall compare it with the total experimentally measured cross section equal to 0.5 mb. This gives the following result for the $\pi\pi KK$ four-branch vertex in the annihilation channel

$$\int |A_{\pi\pi KK}^{\text{ann}} / 16\pi|^2 d\Omega_{\text{ann}} / 4\pi \approx \frac{1}{4}, \quad \sigma_{\pi\pi}^{\text{ann}} \approx 2 \text{ mb} \quad (7)$$

*It should be noted that formula (6') is applicable for the region of the spectrum $\omega_- \leq \omega \leq \omega_+$, where

$$2E^2 \omega_{\pm} = (m_0 + \omega_0)(E^2 + m^2 - (\mu_1 + \mu_2)^2) \\ \pm p_0 \sqrt{[E^2 - (m + \mu_1 + \mu_2)^2][E^2 - (m - \mu_1 - \mu_2)^2]},$$

$$E^2 = m_0^2 + \mu_0^2 + 2m_0\omega_0.$$

For some values of the particle mass, values $m \leq \omega < \omega_-$ are permissible, i.e., not all kinematically possible energy values are realized in the region under consideration. For $m \leq \omega < \omega_-$, we should, in such a case, subtract from (6') a similar term, substituting

$$s_m \rightarrow -2p_0 \sqrt{\omega^2 - m^2} + m_0^2 + m^2 + \mu_0^2 + 2m_0\omega_0 - 2\omega(m_0 + \omega_0).$$

†Thus, e.g., the mean values of the energy \bar{T} according to the theoretical and experimental spectrum for prongless and one-prong stars are equal to 1.45 and 1.60 Bev respectively. \bar{T} taken from the phase curve equals 1.15 Bev.

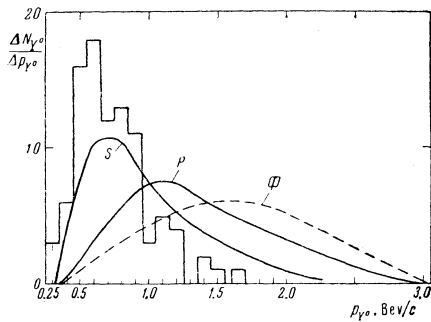


FIG. 6. Momentum spectrum in the l.s. of hyperons for: S – scalar, P – pseudoscalar; Φ – phase volume curve.

and corresponds to the region in which the square of the energy s varies in the range $4\mu_K^2 \leq s \leq 2.5 \times m_N^2$ (the kinetic energy of K^0 and \bar{K}^0 mesons in their c.m.s. $T_{c.m.s.} \approx 0.5$ Bev). It is evident that we can disregard the assumption $\int |A_{\pi^-\pi^+}^{ann}| \times d\Omega_{ann} = \text{const.}$, in which case the estimate obtained will signify some value averaged over the energy interval in the annihilation channel $T_{c.m.s.} \approx 0.5$ Bev.

We can consider the process of hyperon production (2') in a similar way. In this case, the polar contribution (Fig. 5) is given by the cross section for the process (4)

$$\sigma_{\pi K}^{sc}(s') = (4/s') \int |A_{\pi\pi KK}^{sc} / 16\pi|^2 d\Omega_{sc}, \quad (8)$$

equal to half the sum of the cross section for the elastic scattering and charge exchange (s' is the square of the total energy in the c.m.s. for the same process). For simplicity, we shall again assume that $\int |A^2| d\Omega_{sc} = \text{const.}$ and, depending on the parities in the polar diagrams of the vertices NYK, we shall consider three possible variants: 1) NAK and $N\bar{\Sigma}K$ are scalar, 2) NAK and $N\bar{\Sigma}K$ are pseudoscalar, and 3) NAK and $N\bar{\Sigma}K$ have different parities.

Figure 6 shows the momentum spectra of hyperons in the l.s. for variants 1 and 2, and also the spectrum corresponding to the curve of the phase space (6'). The curve for variant 3 has a form intermediate between that of 1 and 2 varying with the ratio of the constant $g_{\Sigma}^2/g_{\Lambda}^2$. For the scalar variant, the theoretical spectrum is in agreement with the experimental one. The variants 2 and 3 give harder spectra. This shows that, for a pseudoscalar interaction, the nonpolar diagram should contribute more at least for $p \gtrsim m_N$ ($|t| \gtrsim m^2$), since, without this contribution, it is impossible to explain the fast decrease of the spectrum in the range $p \gtrsim 0.7$ Bev. For the same reason, we shall compare the integral cross sections over the range $p \leq 0.7$ Bev, which encompasses about half of the hyperons (~ 0.25 mb).

This leads to the following values of the $\pi\pi KK$ four-branch vertex in the scattering channel for the different variants:

$$\begin{aligned} 1) \quad & \int |A_{\pi\pi KK}^{sc} / 16\pi|^2 d\Omega_{sc} / 4\pi \approx 1.7 / [g_{\Lambda}^2(S) + g_{\Sigma}^2(S)], \\ 2) \quad & \int |A_{\pi\pi KK}^{sc} / 16\pi|^2 d\Omega_{sc} / 4\pi \approx 30 / [g_{\Lambda}^2(P) + g_{\Sigma}^2(P)], \\ 3) \quad & \int |A_{\pi\pi KK}^{sc} / 16\pi|^2 d\Omega_{sc} / 4\pi \approx 1.7 / [g^2(S) + g^2(P)/17] \end{aligned} \quad (9)$$

and corresponds to the range of variation of the square of the energy $(\mu_K + \mu)^2 \leq s' \leq 1.5 m_N^2$ (kinetic energy in the c.m.s. $T'_{c.m.s.} \approx 0.5$ Bev).

For variants 1 and 2, only the top limits of the interaction constants are at present established:¹⁴

$$g_{\Lambda}^2(S) = g_{\Sigma}^2(S) < 0.6, \quad g_{\Lambda}^2(P) = g_{\Sigma}^2(P) < 10,$$

which leads to the cross section averaged over the interval $T'_{c.m.s.} \approx 0.5$ Bev

$$\bar{\sigma}_{\pi\pi}^{sc} \gtrsim 30 \text{ mb (variants 1 and 2)}. \quad (10)$$

For the variant 3, even softer top limits are obtained, which leads to a cross section

$$\bar{\sigma}_{\pi\pi}^{sc} \gtrsim 10 \text{ mb (variant 3)}. \quad (11)$$

The results (10) and (11) are in agreement with the estimate of the cross section of πK scattering for $T'_{c.m.s.} \approx 0$ obtained earlier in an analogous manner.¹⁶ If, however, the constants of the NYK interaction are several times less than the limiting values used by us, then the amplitudes (9) would lead to rather high values for the cross section for πK scattering.

In conclusion, we shall briefly discuss the possible contributions from nonpolar diagrams neglected in the above approximation. The pole spectra for the reaction (1') (see Fig. 2) and for the scalar variant of reaction (2') (see Fig. 6) are in agreement with experimental data, and yet differ significantly from the phase curve (6') because of an additional dependence of the polar amplitude on the transferred momentum t . Similarly, there is no reason to assume large contributions from nonpolar amplitudes, since otherwise the nonpolar amplitudes should, in the physical range, have the same dependence on t as the polar amplitudes. It is interesting to note that an analogous situation also occurs in a number of other experiments at high energies reported at the 10th Conference on High-Energy Particle Physics, Rochester, 1960. However, it should be mentioned that the range $t \approx -m_N^2/2$ corresponding to the mean part of experimentally measured baryon spectra is far from the poles $t = \mu^2$ for (1') and $t = \mu_K^2$ for (2'), so that the polar amplitudes are in this case already not large and do not depend strongly on t .

In contrast to the cases studied, it is necessary to assume a contribution from nonpolar diagrams for pseudoscalar variants of reaction (2') in order that the sum of polar and nonpolar contributions should have a sufficiently strong variation for $t \gtrsim -m_N^2$ and give a decreasing experimental spectrum in the interval $-m_N^2/2 \gtrsim t > -m_N^2$. To this end, it turns out to be necessary to introduce two constant amplitudes independent of t (nonpolar amplitudes for two possible spin invariants γ_5 and $\gamma_5 \hat{p}_0$). We can assume that nonpolar amplitudes are not much greater than the polar ones. In such a case, the values obtained for the cross section of πK scattering may vary by several times.

In conclusion, we express our gratitude to Academician A. I. Alikhanov for helpful advice, to Academician V. I. Veksler who made it possible to carry out the experiments, to I. Ya. Pomeranchuk for discussion of the results, and to Yu. S. Krestnikov, V. P. Rumyantseva, N. S. Khropov, and Yu. I. Makarov for help in the experiment.

¹ Eisler, Plano, Prodell, Samios, Schwart, and Steinberger, *Nuovo cimento* **10**, 468 (1958).

² Proceedings of the 1958 Annual International Conference on High-Energy Physics at CERN, edited by B. Ferretti, Geneva, CERN Scientific Information Service, 1958, p. 147.

³ Bowen, Hardy, Reynolds, Sun, Tagliari, Werbrouck, and Moore, *Phys. Rev.* **119**, 2130 (1960).

⁴ Slaughter, Harth, and Block, *Phys. Rev.* **109**, 2111 (1958).

⁵ Blumenfeld, Chinowsky, and Lederman, *Nuovo cimento* **13**, 296 (1958).

⁶ Kuznetsov, Ivanovskaya, Prokesh, and Chuvilo, Proceedings of the 1960 Annual International Conference on High-Energy Physics at Rochester, University of Rochester, 1960, p. 382.

⁷ Wang, Wang, Veksler, Vrana, Ding, Ivanov, Kladnitskaya, Kuznetsov, Nguen, Nikitin, Solov'ev, and Ch'eng, *JETP* **40**, 464 (1961), *Soviet Phys. JETP* **13**, 323 (1961).

⁸ Blinov, Lomanov, Meshkovskii, Shalamov, and Shebanov, *Приборы и техника эксперимента (Instruments and Exptl. Techniques)* No. 1, 35 (1958).

⁹ L. B. Leipuner, Some Relativistic Two Body Kinematics Tables, Brookhaven National Laboratory, 1958.

¹⁰ Crawford Jr., Cresti, Cood, Solmitz, Stevenson, and Ticho, *Phys. Rev. Lett.* **2**, 174 (1959); W. L. Alvarez, Proc. High-Energy Physics Conf., Kiev, 1959.

¹¹ G. F. Chew and F. E. Low, *Phys. Rev.* **113**, 1640 (1959).

¹² L. B. Okun' and I. Ya. Pomeranchuk, *JETP* **36**, 300 (1959), *Soviet Phys. JETP* **9**, 207 (1959).

¹³ V. B. Berestetskii and I. Ya. Pomeranchuk, *JETP* **39**, 1078 (1960), *Soviet Phys. JETP* **12**, 752 (1960).

¹⁴ Kycia, Kerth, and Baender, *Phys. Rev.* **118**, 553 (1960).

¹⁵ Ya. I. Granovskii and V. N. Starikov, *JETP* **40**, 537 (1961), *Soviet Phys. JETP* **13**, 375 (1961).

¹⁶ G. Kosta and L. Tenaglia, *Nuovo cimento* **18**, 368 (1960).